Rapid transport of neural intermediate filament protein

Brian T. Helfand*, Patty Loomis*, Miri Yoon and Robert D. Goldman‡

Department of Cell and Molecular Biology, Northwestern University Feinberg School of Medicine, 303 East Chicago Avenue, Ward 11-145, Chicago, IL 60611, USA

*These authors contributed equally to this work

‡Author for correspondence (e-mail: r-goldman@northwestern.edu)

Accepted 1 April 2003
Journal of Cell Science 116, 2345-2359 © 2003 The Company of Biologists Ltd
doi:10.1242/jcs.00526

Summary

Peripherin is a neural intermediate filament protein that is expressed in peripheral and enteric neurons, as well as in PC12 cells. A determination of the motile properties of peripherin has been undertaken in PC12 cells during different stages of neurite outgrowth. The results reveal that non-filamentous, non-membrane bound peripherin particles and short peripherin intermediate filaments, termed 'squiggles', are transported at high speed throughout PC12 cell bodies, neurites and growth cones. These movements are bi-directional, and the majority require microtubules along with their associated molecular motors, conventional kinesin and cytoplasmic dynein. Our data demonstrate that peripherin particles and squiggles can move as components of a rapid transport system capable of delivering cytoskeletal subunits to the most distal regions of neurites over relatively short time periods.

Movies available online

Key words: Intermediate filaments, Peripherin, Dynein, Kinesin, Cytoskeleton

Introduction

The morphology of the typical neuron consists of a cell body with unusually long cytoplasmic processes. The longest of these is the axon. As a consequence of these morphological features, the volume of the 'axoplasm' frequently exceeds the volume of the cytoplasm in the cell body many fold. Since most protein synthesis takes place in the cell body, the neuron must move vital materials made in this region to the most distal parts of axons using an elaborate transport system consisting of both fast and slow moving components (Hammerschlag et al., 1994; Hoffman and Lasek, 1975; Lasek and Hoffman, 1976). To date, only membrane-bound organelles such as mitochondria, Golgi vesicles and lysosomes are known to move as fast components (50-400 mm/day) (Brown, 2000). In contrast, cytoskeletal components including intermediate filaments (IF), microfilaments, microtubules (MT), as well as their structural subunits, appear to move at slow rates of ~0.3-8 mm/day (Brown, 2000). At these rates, it could take months or even years for the subunits of cytoskeletal proteins to turnover in the most distal regions of axons, which can be several meters long. In light of the known dynamic properties of each of these cytoskeletal systems, it would be surprising if the turnover of all of their structural subunits took place at such slow rates. This is especially the case for neural IF, which in many neurons are the major protein components of axons (Nixon, 1993).

Recently, observations of neurons expressing either type IV IF GFP-tagged neurofilament (NF) medium (GFP-NF-M) or heavy (GFP-NF-H) subunits, revealed that short IF can move at rates up to ~1.8 μm/second in vivo. However, since these NF spend 73-80% of their time not moving, they remain categorized as components of slow axonal transport (Roy et al., 2000; Wang and Brown, 2001; Wang et al., 2000). It has also been shown that non-membrane bound particles containing non-filamentous forms of NF proteins and kinesin can move rapidly along MT in cell-free preparations of squid axoplasm (Prahlad et al., 2000). Similarly, in extracts of bovine spinal cord, NF have been reported to move rapidly along MT in association with cytoplasmic dynein and kinesin (Shah et al., 2000). However, since pause times were not determined in either of these in vitro studies, it is possible that these movements may also reflect stationary periods punctuated by rapid movements.

Direct observations of the motile properties of IF in non-neuronal cells such as those expressing GFP-tagged vimentin, a type III IF protein, have revealed a surprisingly wide range of movements (Ho et al., 1998; Prahlad et al., 1998; Yoon et al., 1998). This was especially evident in spreading cells in which large numbers of vimentin particles move in both retrograde and anterograde directions at speeds >1.0 μm/second (Prahlad et al., 1998). These particles frequently form short filamentous structures termed squiggles, which subsequently become incorporated into the longer IF that typify fully spread fibroblasts. The rapid movements exhibited by vimentin particles are dependent upon MT, conventional kinesin and cytoplasmic dynein (Helfand et al., 2002; Prahlad et al., 1998).

On the basis of these observations, it was of interest to determine whether similar types of rapidly moving IF particles and squiggles could provide a mechanism for the timely turnover of IF subunits in the most distal regions of axons. In this study we describe the transport of the type III IF protein peripherin in differentiating PC12 cells, a widely used model

for studies of sympathetic neurons (Fujita et al., 1989). Peripherin is the major IF protein present in PC12 cells and small caliber, non-myelinated neurons of the PNS (Brody et al., 1989; Escurat et al., 1990; Parysek and Goldman, 1988; Troy et al., 1990a). Our results demonstrate that non-membrane bound peripherin particles and squiggles move bi-directionally along neurites as components of a rapid transit system capable of delivering cytoskeletal proteins to all regions of neurons over relatively short time periods. The results are discussed in light of various models for the transport and turnover of neuronal cytoskeletal proteins.

Materials and Methods

Cell culture

Stock cultures of PC12 cells were maintained in Complete Medium (CM; DMEM containing 10% calf serum and 1 mM sodium pyruvate) at 37°C. For some studies of peripherin IF, cells from stock cultures were transferred to Differentiation Medium [DM; DMEM containing 5% calf serum, 1 mM sodium pyruvate and 30 ng/ml of nerve growth factor (NGF, Roche)] for 24 hours. Cells were then removed with Trypsin-EDTA (Gibco-BRL), re-plated onto laminin (Roche) coated coverslips and maintained for 0.5-72 hours in DM prior to analysis. BHK-21 cells were grown as previously described (Prahlad et al., 1998).

Antibodies

Rabbit anti-peripherin (Parysek and Goldman, 1988), anti-dynein heavy chain (HC) and light intermediate chains 1 and 2 [LIC 1 and 2; provided by Richard Vallee, Columbia University (Helfand et al., 2002; Tynan et al., 2000)], Arp-1 [a gift of David Meyer, UCLA (Troy et al., 1990b)] and anti-kinesin [PCP42; provided by Ron Vale, UCSF (Prahlad et al., 1998)] were used. Mouse monoclonal anti-β-tubulin (TU 27B, provided by Lester Binder, Northwestern University), anti-dynein intermediate chain (IC; Chemicon International, Inc.), anti-p150*Glued* and dynamitin (BD Biosciences), and anti-kinesin heavy chain (H1, Chemicon) were also employed. Other antibodies included mouse monoclonal anti-c-myc (Evan et al., 1985) and anti-GFP (clones 7.1 and 13.1; Roche).

FITC-, lissamine-rhodamine and Cy5-conjugated goat anti-mouse and anti-rabbit IgG (Jackson ImmunoResearch, West Grove, PA) were employed for indirect immunofluorescence. Peroxidase-conjugated goat anti-rabbit IgG (Jackson ImmunoResearch) was used for immunoblotting. Immunoelectron microscopy was carried out by using 18 nm gold particles conjugated to goat anti-rabbit IgG (Jackson Immunoresearch) and 10 nm gold particles conjugated to goat anti-mouse IgG (Sigma).

Immunofluorescence

PC12 cells grown on laminin-coated coverslips were rinsed in PBS and fixed in either methanol (Mallinckrodt; –20°C) for 4 minutes or 3.5% formaldehyde (Tousimis) at room temperature for 5 minutes at different times during neurite extension. Following formaldehyde fixation, cells were permeabilized with 0.05% NP-40 for 5 minutes. Cells were then washed with PBS and processed for indirect immunofluoresence as previously described (Prahlad et al., 1998; Yoon et al., 1998). Following staining, coverslips were washed in PBS and mounted on glass slides in gelvatol containing 100 mg/ml Dabco [1,4-diazabicyclo [2.2.2] octane; Aldrich Chemical (Yoon et al., 1998)]. In some preparations, membrane-bound organelles were stained with $DiOC_6$ or SP-$DiOC_{18}$ (Molecular Probes) at a concentration of 0.1 μg/ml for 20 minutes, and then cells were fixed and processed for indirect immunofluorescence using peripherin antibodies (Spector et al., 1997).

Images of fixed, stained preparations were taken with a Zeiss LSM 510 microscope (Carl Zeiss) (Yoon et al., 1998).

Statistical analysis

The immunofluorescence images of peripherin particles, kinesin and dynein were subjected to statistical tests using a modification of our previously published procedure (Prahlad et al., 2000). These tests were carried out to make certain that these associations were not random. To this end, the total number of pixels within randomly selected cytoplasmic regions were determined in cells prepared for double and triple fluorescence microscopy. Specifically, non-transfected cells were fixed and processed for double label immunofluorescence using either peripherin and kinesin antibodies or peripherin and dynein antibodies (see above). For triple fluorescence observations GFP-peripherin-expressing cells were fixed and stained with anti-dynein and anti-kinesin (see above). For each double and triple fluorescence preparation, one cytoplasmic region from each of 10 different cells (a total of 30 cells) was used for the statistical analyses. After normalizing for differences in magnification, it was determined that the average number of pixels per peripherin particle was 41.5±15.0 (n=300), the average number of pixels per kinesin particle was 43.0±13.2 (n=200), and the average number of pixels per dynein particle was 41.9±16.9 (n=200). For the purposes of our calculations we assumed that the particles were circular and that there was extensive overlap between or among the different antibody staining patterns.

For double fluorescence images, the following formula was used to calculate the expected number of peripherin particles (E_{db}) that would coincide with either kinesin or dynein based on chance alone.

$$E_{db} = N_P[(N_m\pi r_m^2)/T],$$

where N_p is the total number of peripherin particles in a cytoplasmic region; N_m is the average number of particles of motor protein (either kinesin or dynein) in a cytoplasmic region; r_m is the average radius (in pixels) of a motor particle; T is the total number of pixels counted in a given cytoplasmic region.

The following formula was used for statistical analyses of triple fluorescence images:

$$E_{tr} = N_D[(E_{db}\pi r_{pk}^2)/T],$$

where E_{tr} is the total number of dynein particles that would be expected to be associated with both peripherin and kinesin by chance alone; E_{db} is the expected number of peripherin particles that would associate with kinesin by chance alone; N_D is the total number of dynein particles in a cytoplasmic region; r_{pk} is the average radius (in pixels) of a peripherin and kinesin doublet; and T is the total number of pixels counted in a given cytoplasmic region.

The number of associations actually observed was also determined for each image. This was defined as the number of peripherin particles that were observed to associate with kinesin and/or dynein. Finally, a two-tailed Student's t-test was used to determine if the differences between the actual and expected values were statistically significant (P<0.001).

Transfection

Rat peripherin cDNA (provided by Linda Parysek, University of Cincinnati) was amplified by PCR using primers that insert *Bam*HI sites at the 5′ and 3′ ends. The resulting *Bam*HI-*Bam*HI fragment was subcloned into the *Bam*HI site of pEGFP-C1 (Clontech). The preparation of GFP-vimentin cDNA and the myc-dynamitin construct has been described elsewhere (Helfand et al., 2002; Yoon et al., 1998). The GFP-peripherin construct was introduced into PC12 cells by electroporation (Yoon et al., 2001), and myc-dynamitin cDNA was introduced by lipofectamine delivery [Gibco (Yoon et al., 1998)]. In some experiments, PC12 cells were mock

transfected with the pCMV-myc vector (Clontech) as a control. Following electroporation, cells were plated on laminin-coated coverslips in CM or DM (see above) and used for live cell analysis within 48-72 hours of transfection. BHK-21 cells were also analyzed 48-72 hours after transfection with GFP-vimentin cDNA as previously described (Prahlad et al., 1998).

Live cell imaging

PC12 cells expressing GFP-peripherin were trypsinized, plated onto laminin-coated coverslips, mounted on glass slides and sealed as previously described (Yoon et al., 1998). The culture medium used in these preparations was Leibovitz L-15 (Gibco/BRL) containing 5% calf serum, 1 mM sodium pyruvate and 30 ng/ml NGF. Cells were maintained at 37°C during microscopic examination with an air stream incubator (NEVTEK). In some experiments cells were treated with colchicine (5 μg/ml; Sigma) in DM for 30-90 minutes. Under these conditions, no microtubules could be detected by indirect immunofluorescence within 15-30 minutes (data not shown).

Time-lapse observations were made using a Zeiss LSM 510 confocal microscope as previously described (Yoon et al., 1998). Images were captured at ~5 second intervals at a resolution of 512×512 dots per inch with a scanning time of ~1 second. Images were collected for ~5-30 minute time periods. Analyses of peripherin particle and squiggle motility were carried out in PC12 cells at different times within 0.5-72 hours of trypsinization and replating in DM (see above). Analyses of vimentin particle motility in BHK-21 cells were carried out in the peripheral regions of interphase cells. In both cell types, rates of translocation of particles and squiggles were obtained by monitoring distance traveled during the 5 second intervals between capturing images using Metamorph image analysis software (Universal Imaging Corp.) as previously described (Yoon et al., 1998). Since the movements were discontinuous, pause times were also determined (Wang et al., 2000). The pause time was defined as a 6 second interval during which a particle or squiggle moved less than 0.5 μm.

Fluorescence recovery after photobleaching (FRAP) analyses were carried out on the neurites of differentiated cells expressing GFP-peripherin at 48 hours, using the Zeiss LSM 510 microscope as previously described (Yoon et al., 1998). For this purpose only one neurite was placed in the microscope field of view using a 100× oil immersion (1.4 NA, plan-apochromatic lens). In some experiments, ~8-10 μm^2 areas were bleached along the long axes of neurites and recovery was monitored. In other experiments, larger regions (~35-50 μm^2) were bleached. Owing to the size of the bleach zone relative to the total area of the single fluorescent neurite within the field of view, the gray-scale pixel values of the bleach zone were normalized by dividing by the gray scale pixel values of the same sized regions in control (unbleached) areas (the F.I. ratio) of the same neurite using LSM510 imaging software. In order to analyze the details of fluorescence recovery in these large bleach zones, the F.I. ratio was first determined for the overall bleach zone and subsequently for 1 μm subdomains of the entire area. In some FRAP experiments, colchicine was added at 5 μg/ml in DM 15 minutes prior to observation. In several experiments, cells were processed for immunofluorescence with peripherin antibody (see above) on the microscope stage to determine whether peripherin fibrils were present within the bleach zone.

Neurite outgrowth was monitored after cells were plated in DM on locator coverslips (Bellco). Subsequently, phase images were taken of the same 100 cells at 6, 12, 24, 48 and 72 hours. Measurements of neurite length at each time interval were made with Zeiss LSM 510 imaging software.

IF-enriched cytoskeletal preparations

IF-enriched cytoskeletal preparations were made from subconfluent cultures of transfected PC12 cells grown in DM for 24 hours as previously described (Zackroff et al., 1982). These preparations were analyzed by SDS-PAGE (Laemmli, 1970). The separated proteins were transferred to nitrocellulose for immunoblotting (Towbin et al., 1979). All antibody incubations were carried out in PBS containing 5% non-fat dry milk (Sigma).

Platinum replica electron microscopy

PC12 cells were grown in DM for 24-48 hours. Two hours before processing, cells were trypsinized and replated onto laminin-coated coverslips in DM. Ultrastructural observations of cytoskeletal preparations were performed as described elsewhere (Svitkina et al., 1995). Briefly, cells on coverslips were extracted with PEM buffer (100 mM PIPES, pH 6.9, 1 mM $MgCl_2$, 1 mM EGTA) containing 1% Triton X-100, 4% polyethylene glycol (PEG) for 5 minutes. In some experiments 10 μg/ml Taxol (Sigma) was added to the PEM buffer solution to preserve MT integrity. In these experiments, actin was removed by adding 1 mg/ml DNase 1 to the PEM buffer and by incubating PC12 cytoskeletons with recombinant gelsolin N-terminal domain [provided by Gary Borisy, Northwestern University (Verkhovsky and Borisy, 1993)]. In other experiments, 2 mM phalloidin (Molecular Probes) was added to the PEM buffer to preserve actin structures. These preparations were then fixed with 2% glutaraldehyde, labeled with gold-conjugated antibodies, stained with 0.1% tannic acid/0.2% uranyl acetate and processed by critical point drying/rotary shadowing as previously described (Helfand et al., 2002; Svitkina et al., 1995). Controls for these preparations involved all of the various steps and incubations described above using either no antibodies or secondary gold-coupled antibodies alone.

Microinjection

PC12 cells growing in DM on locator coverslips (Bellco) were selected using a Zeiss axiomat inverted microscope. Antibodies directed against kinesin heavy chain (H1; Chemicon) or control preimmune IgG (5 mg/ml) were dialyzed into microinjection buffer (20 mM Tris, pH 7.5 in 75 mM NaCl), clarified by centrifugation and then microinjected into the selected cells (Prahlad et al., 1998). Injected cells were fixed and processed for immunofluorescence within 0.5-4 hours.

Results

Peripherin patterns during neurite outgrowth

The organization of peripherin in PC12 cells was studied by immunofluorescence at 30-60 minutes following replating in DM. At this time the cells appeared fibroblastic in shape and neurite outgrowth was not evident. Peripherin was organized into numerous particles, squiggles and longer filamentous structures. These structures were most evident in the peripheral regions of the cytoplasm (Fig. 1A-C). After 2 hours, early neurite outgrowth was detected in most cells. At this time, there was an apparent increase in both the number and length of IF in the cell bodies and extending neurites (Fig. 1D). Growth cones also contained peripherin particles, squiggles and some longer filaments (Fig. 1E-F). Particles could also be detected in the most distal regions containing filopodia (see Fig. 2A-G). After 24-72 hours in DM, neither particles nor squiggles were evident in cell bodies and neurites, although the large number of peripherin IF may have obscured them. However, both forms of peripherin were readily detectable in growth cones (Fig. 1G-I). Double staining of cells with the lipophilic dyes, $DiOC_6$ or SP-$DiOC_{18}$, and anti-peripherin demonstrated that the particles were not membrane-bound (data not shown; see Materials and Methods).

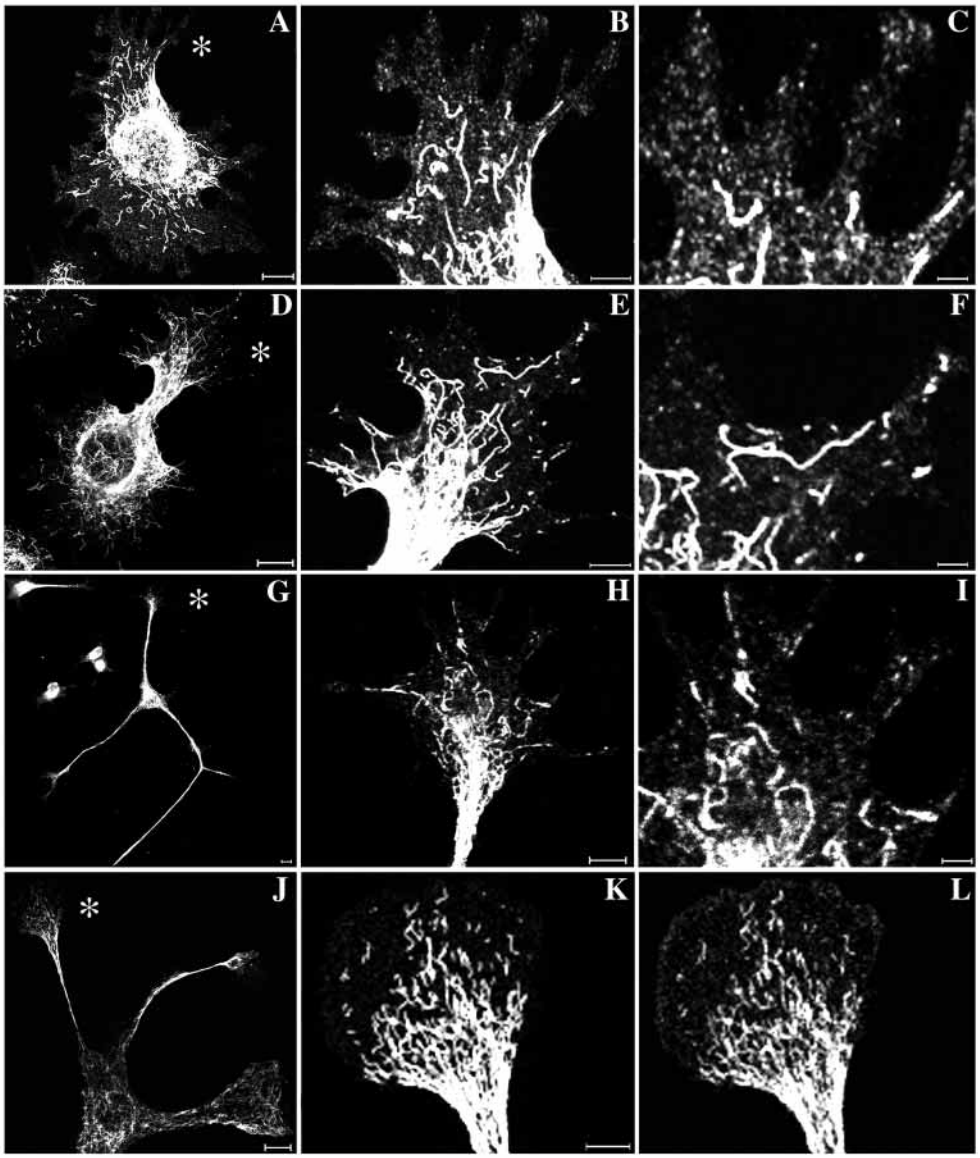

Fig. 1. Peripherin particles, squiggles and longer IF. PC12 cells were fixed and processed for immunofluorescence at 0.5 hours (A-C), 2 hours (D-F) and 24 hours (G-I) after plating in DM. Peripherin particles and squiggles were apparent in regions between the nucleus and the cell surface between 0.5 and 2 hours (A-F; B and C are higher magnification views of the region denoted by the * in A; E and F are higher magnification views of the region indicated by the * in D). Longer IF were also present during this period. Growth cones and early neuritic processes, evident at ~2 hours, also contained particles and squiggles (D-F). After 24 hours, a large number of longer peripherin IF were present in most regions of differentiated cells, and particles and squiggles were most obvious in growth cones [G-I; the growth cone region (*) in G is seen at higher magnifcations in H and I]. Panels J-L show GFP-peripherin in a cell fixed at 2 hours in DM. The GFP fluorescence is observed directly in J-K, and peripherin is observed indirectly by anti-peripherin stained with lissamine-rhodamine-conjugated goat anti-rabbit in L. The * in J represents the growth cone region seen in K and L. Bar, 10 μm in A,D,G,J; Bar, 5 μm in B,E,H,K,L; Bar, 2 μm in C,F,I.

Platinum replica immunogold electron microscopic analyses revealed clusters of gold corresponding to the peripherin particles. These were most obvious in growth cones in close association with the dense actin networks found in these regions as well as the actin bundles in filopods (Fig. 2D-E). Short and longer linear arrays of gold-conjugated antibodies corresponding to the peripherin squiggles and longer IF observed by immunofluorescence were present within the central region of growth cones and in neurites (Fig. 2F-G; and data not shown). No gold labeling was observed in control cells (see Materials and Methods; data not shown). These observations confirm the presence of the different forms of peripherin seen by light microscopy.

We also determined whether the same IF patterns were seen during neurite outgrowth in GFP-peripherin-expressing PC12 cells grown in DM for periods up to 72 hours. Direct observations of GFP-peripherin fluorescence patterns in these cells was indistinguishable from those seen at the same time intervals in non-transfected cells (e.g., 2 hours; Fig. 1J-L and data not shown). Further evidence supporting the incorporation of GFP-peripherin into endogenous peripherin structures was derived from SDS-PAGE and immunoblotting of IF- enriched cytoskeletal preparations made from cultures containing ~70% GFP-peripherin-transfected PC12 cells (Zackroff et al., 1982). The results showed that peripherin and an 85 kDa band corresponding to GFP-peripherin were present in the endogenous IF system (Fig. 3).

Fast transport of peripherin

Since non-transfected and GFP-peripherin transfected PC12 cells exhibited indistinguishable patterns and assembly states of IF protein, we next determined the properties of peripherin in vivo. Live cells expressing GFP-peripherin were observed at time intervals after trypsinization and replating into DM. At early time points (0.5-6 hours), peripherin particles and squiggles were observed to move in all regions of the cytoplasm including cell bodies, neurites and growth cones (see Fig. 4A-D and Movie 1). Numerous peripherin particles could also be seen using phase contrast microscopy (see arrowheads in Fig. 2A-C).

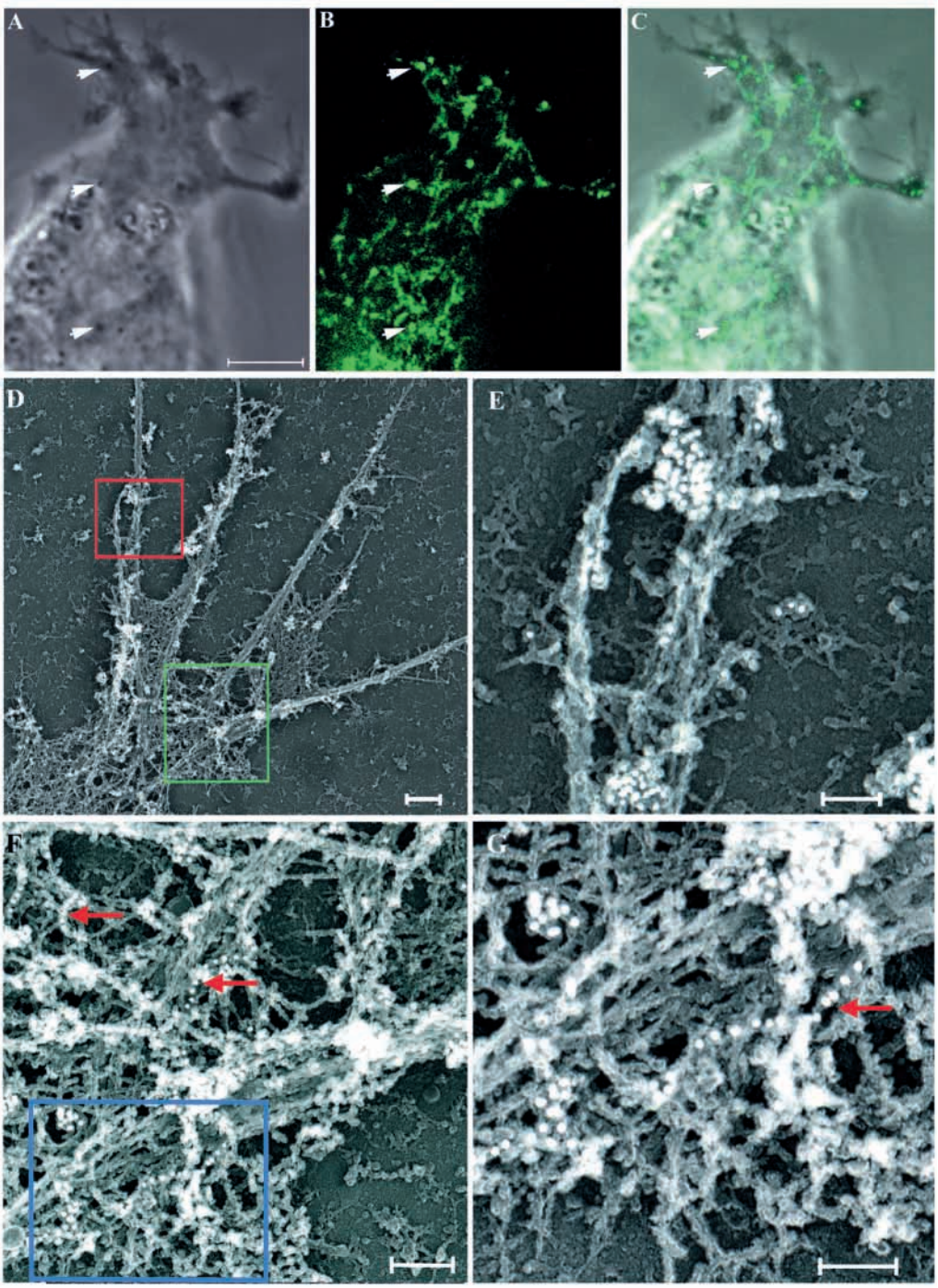

Fig. 2. Peripherin is present in growth cones. A living PC12 cell expressing GFP-peripherin during the early stages of neurite outgrowth. This cell was observed at ~1-2 hours after plating in DM. Numerous GFP-peripherin particles and squiggles can be seen within the growth cone. A-C represents a single image from a time-lapse series. The image was captured by both phase-contrast and fluorescence microscopy to show the relationships between particles, squiggles, growth cones and filopodial extensions. The arrowheads indicate the positions of peripherin particles, some of which can also be detected with phase contrast. The particles and squiggles seen in the growth cone region are motile (see Movie 1 at jcs.biologists.org/supplemental). Bar, 5 μm in A-C. PC12 cells were plated in DM for 2 hours and then processed for platinum-replica immunogold TEM as described in Materials and Methods using rabbit anti-peripherin and gold-conjugated secondary antibodies. Ultrastructural observations (D-E) demonstrate that peripherin particles are present within the actin-rich growth cones and filopodia. In more proximal regions of growth cones, peripherin particles (indicated by clusters of 18 nm gold), as well as peripherin squiggles (most probably represented by linear arrays of gold; see arrows), are readily observed (F,G). E is a higher magnification view of area in the red box in D; F is a higher magnification view of the area in the green box in D; and G is a higher magnification view of the area in the blue box in F. Bar, 100 nm in D,E,G; Bar, 500 nm in F.

The rates of peripherin particle translocation were determined in cells 0.5-2 hours after replating in DM (see Materials and Methods), prior to the formation of distinct neurites. Approximately 72% of these particles moved (*n*=50; see Table 1). Of these particles, almost half exhibited ‘reversals’; that is, an individual particle moved first in one direction and then in the opposite direction (see Table 1). However, the majority of the movements (~75%) were directed towards the cell surface (anterograde) at rates ranging from 0.08-1.45 μm/second (averaging 0.34±0.21 μm/second; Table 1). Particles moving towards the nucleus (retrograde) moved at rates ranging from 0.08-1.20 μm/second (averaging 0.34±0.24 μm/second; Table 1). Calculation of pause times (see Materials and Methods) revealed that the particles moved ~46% of the time. These movements were similar to vimentin particle motility in peripheral regions of spread BHK-21 cells (Table 1).

Peripherin squiggles were also studied in PC12 cells within 0.5-2 hours in DM. Overall their movements were similar to those described for particles at the same time points (Fig. 4F; Table 1). Approximately 35% of all of the squiggles (*n*=64) moved, mainly anterograde, at rates ranging from 0.08 to 1.14 μm/second (averaging 0.40±0.25 μm/second; Table 1). Retrograde rates ranged from 0.08 to 1.22 μm/second

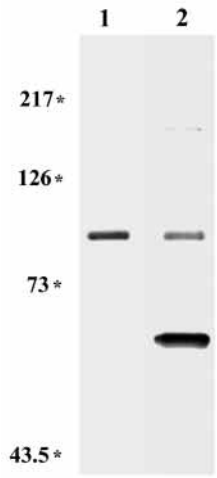

Fig. 3. GFP-Peripherin is incorporated into endogenous IF. Analysis of IF-enriched cytoskeletal preparations of GFP-peripherin transfected PC12 cells. 2 μg/lane of an IF-enriched cytoskeletal extract from GFP-peripherin-transfected PC12 cells was separated by SDS-PAGE and immunoblotted with either anti-GFP (Lane 1) or anti-peripherin (Lane 2). The GFP antibody detects a single band at 84 kDa representing GFP-peripherin whereas the peripherin antibody detects both GFP-peripherin and the 57 kDa endogenous peripherin. Molecular weight standards are indicated at left.

(averaging 0.38±0.28 μm/second; Table 1). Furthermore, a calculation of their pause rates showed that they moved ~68% of the observation period (Table 1).

As mentioned above, differentiated PC12 cells grown in the presence of NGF for 24-72 hours exhibit dense networks of peripherin IF throughout their cell bodies and neurites. In these cells, particle and squiggle motility was only evident in the peripheral regions of the cell body and growth cones (see Fig. 4A-E,G,H). In the cell body, ~67% (*n*=50) of the particles moved with rates similar to those seen at earlier time points in DM (Table 1). The net translocation of >55% of these particles was anterograde, even though half of the particles reversed directions at least once during the observation period (Table 1). Particles moved at rates between 0.08-1.11 μm/second (averaging 0.31±0.20 μm/ second; Table 1) in the anterograde direction, and in the retrograde direction between 0.08-1.14 μm/second (averaging 0.30±0.22 μm/second; Table 1). Analyses of the movements of peripherin squiggles in cell bodies revealed that they moved ~63% of the time (Table 1). Of these movements, ~62% were directed towards the cell surface at rates ranging from 0.08-1.09 μm/second (averaging 0.41±0.24 μm/second; Table 1), and ~38% of the movements were in the retrograde direction at rates of 0.08-1.25 μm/second (averaging 0.34±0.23 μm/second; Table 1). Many squiggles were also observed to change directions (Fig. 4G; Table 1). It should be noted that the majority of neurite elongation or outgrowth takes place within 12 hours of plating in DM (see Materials and Methods). At this time the average length of neurites is ~48 μm, and after 72 hours it is ~62 μm (*n*=100, data not shown). Therefore, at these time points the rates of neurite outgrowth were minimal and had no significant impact on our measurements of particle and squiggle motility.

In the case of the growth cones of differentiated cells in DM for 24-72 hours (see above), observations were limited to their central domains (Mueller, 1999) where rapid changes in shape do not occur. In this area, particles and squiggles were observed to move ~53% (*n*=50; Table 1) and ~58% (*n*=52; Table 1) of the time, respectively. About half of the particle (~53%; Table 1) and squiggle (~51%; see Table 1) movements were anterograde. The range and average velocities of these peripherin structures were not significantly different from those described above ($P<0.005$, using Student's *t*-test; see Table 1). Similarly, ~50% of the particles and squiggles reversed direction during movement (Fig. 4H; Table 1). Therefore, the motile properties of peripherin particles and squiggles in two major domains of PC12 neurons, cell bodies and growth cones, are similar. In addition, these properties are also very similar to those found for vimentin in BHK-21 fibroblasts (Table 1).

It was also of interest to determine the motile properties of peripherin IF in the neurites of extensively differentiated PC12 cells. For this purpose, fluorescence recovery after photobleaching (FRAP) analyses were initially carried out on ~8-10 μm^2 regions along neurites in GFP-transfected cells grown in DM for 48 hours. The time for the bleach zones to completely recover their fluorescence was ~10-14 minutes with an average $t_{1/2}$ of ~5.5 minutes (*n*=8; data not shown). Interestingly, during fluorescence recovery we frequently found that particles and squiggles would rapidly traverse the bleach zones (see Fig. 5E-I, Movie 3, available at jcs.biologists.org/supplemental). In order to observe the movements of these structures in more detail and to determine their contribution to fluorescence recovery, we bleached much larger regions (35-50 μm^2) along the length of neurites (see Fig. 5A1-A3). The overall rate of fluorescence recovery for these larger areas containing longer peripherin IF was similar to that described above (Fig. 5A). However, after dividing these larger photobleach zones into smaller areas of equal size (Fig. 5C1-C3), we frequently detected transient spikes in

Table 1. Analysis of peripherin motility

Time in DM	Cell domain	Particle/ squiggle	Number counted	Time moving (%)	Time pausing (%)	Antero movements (%)	Retro movements (%)	Reversals (%)	Average anterograde motility (μm/sec)	Range anterograde (μm/sec)	Average retrograde motility (μm/sec)	Range retrograde (μm/sec)
PC12 cell 0.5-6 hours DM	Cell body	Particle	50	46	54	75	25	46	0.34±0.21	0.08-1.45	0.34±0.24	0.08-1.20
PC12 cell 0.5-6 hours DM	Cell body	Squiggle	64	68	32	59	41	20	0.40±0.25	0.08-1.14	0.38±0.28	0.08-1.22
PC12 cell 24-72 hours DM	Cell body	Particle	50	67	33	55	45	50	0.31±0.20	0.08-1.11	0.30±0.22	0.08-1.14
PC12 cell 24-72 hours DM	Cell body	Squiggle	50	63	37	62	38	34	0.41±0.24	0.08-1.09	0.34±0.23	0.08-1.25
PC12 cell 24-72 hours DM	Neurite	Particle	77	75	25	65	35	8	0.33±0.24	0.08-1.45	0.30±0.20	0.08-1.54
PC12 cell 24-72 hours DM	Neurite	Squiggle	50	70	30	62	38	6	0.31±0.29	0.08-1.21	0.30±0.28	0.08-1.00
PC12 cell 24-72 hours DM	Growth cone	Particle	50	53	47	53	47	50	0.35±0.25	0.08-1.19	0.32±0.19	0.08-0.92
PC12 cell 24-72 hours DM	Growth cone	Squiggle	52	58	42	51	49	48	0.32±0.18	0.08-1.05	0.30±0.22	0.08-1.21
BHK-21 Fibroblast*	Cell body	Particle	53	45	55	66	34	36	0.39±0.24	0.08-1.65	0.43±0.26	0.08-1.40

Time-lapse images of GFP-peripherin particles and squiggles in PC12 cells plated in DM for either 0.5-6 hours or 24-72 hours were captured every 5 seconds. A large photobleach zone was made in experiments involving analyses of peripherin motility in neurites (24-72 hours in DM). A pause was defined as no movement or <0.5 μm in 6 seconds. A reversal of movement was defined as an individual particle or squiggle that moved first in one direction and then in the opposite direction. For comparison, the movements of GFP-vimentin particles in well-spread BHK-21 fibroblasts were analyzed in peripheral regions.

*BHK-21 cells were grown as described in Materials and Methods.

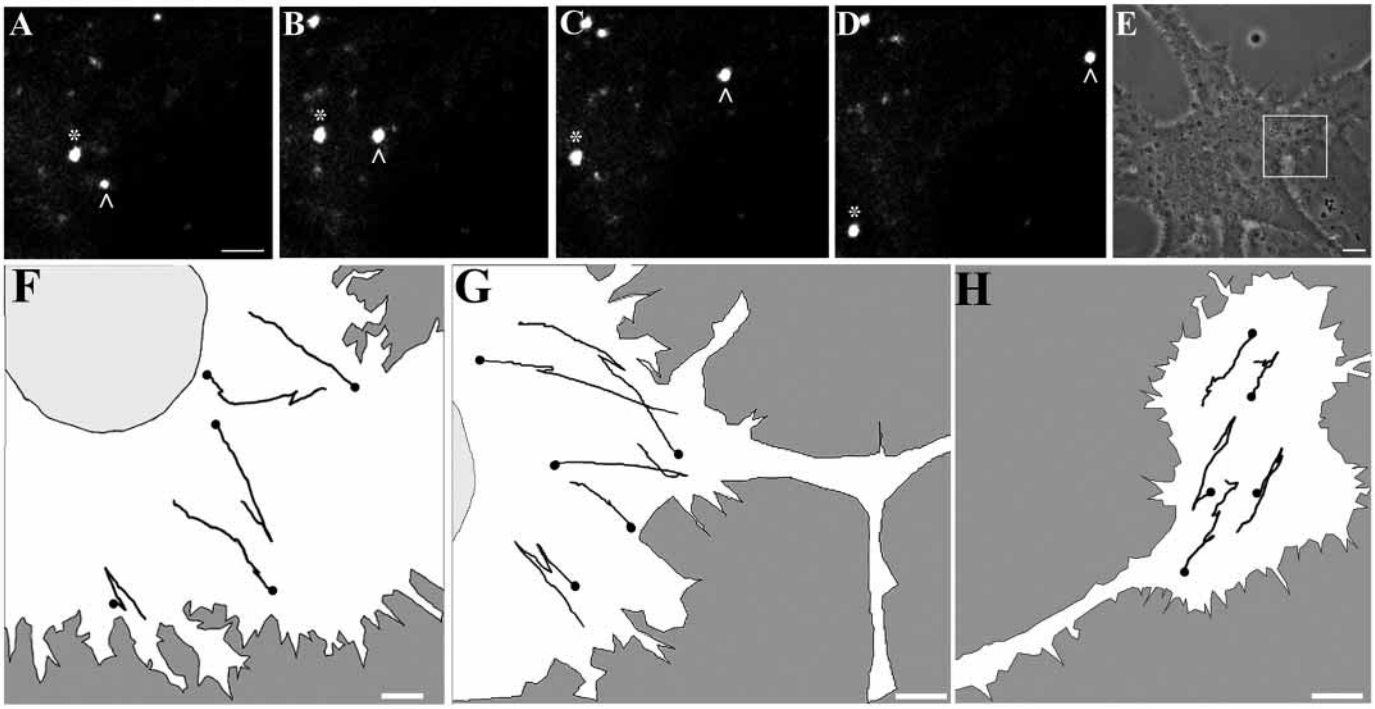

Fig. 4. Peripherin particles and squiggles move rapidly and bi-directionally. Analyses of the motile properties of particles and squiggles were made in GFP-peripherin-transfected cells in DM for periods of 2-4 hours (A-F) and at 48 hours (G,H). Observations were restricted to the peripheral regions of cell bodies and the central domain of growth cones at later time points, as both particles and squiggles were most obvious within these regions. A-E are derived from a time-lapse series (1 frame every 5 seconds) in the region of the cell body indicated by the box in the phase image (E). The particle marked * moved in a retrograde direction, and that marked with the arrowhead moved in an anterograde direction. F-H are diagrammatic representations of the trajectories of individual peripherin squiggles in the cell bodies (F,G) and in a growth cone (H). Black dots represent the beginning of squiggle tracks. A-D, Bar, 2 μm; E-H, Bar, 5 μm.

fluorescence intensity that were much brighter than the intensity recorded just prior to photobleaching (Figs. 5B,C). These spikes were due to the rapid movements of particles and squiggles into and out of bleach zones (Fig. 5B-1 to B-3 and Fig. 5C-1 to C-3). These rapid and bi-directional movements of particles and squiggles became evident only during the period preceding the recovery of dense peripherin networks (see Movie 3 at jcs.biologists.org/supplemental).

We also determined the rates and directions of movements of particles and squiggles within neurites after photobleaching at 48 hours in DM and compared their properties to those observed during the early stages of neurite outgrowth (0.5-6 hours, see above). Although particles (n=77) were observed to move into the bleach zone from both ends, the majority of movements were anterograde (~65%; Table 1). The rates of anterograde particle movements ranged from 0.08 to 1.45 μm/second (average of 0.33±0.24 μm/second; Table 1) and retrograde rates were from 0.08 to 1.54 μm/second (average of 0.30±0.20 μm/second; Table 1). Interestingly, very few reversals were observed (Fig. 5J). For example, of the 77 particles studied, only 8% reversed their direction (see Table 1). Determination of pause times revealed that in neurites, peripherin particles moved ~75% of the time.

Further analysis of motile squiggles (n=50) in neurites after 48 hours in DM revealed that ~62% moved in the anterograde direction at rates of 0.08 to 1.21 μm/second (average of 0.31±0.29 μm/second; Table 1). Retrograde movements ranged from 0.08-1.0 μm/second (average of 0.30±0.28 μm/second; Table 1). Calculation of pause times demonstrated that squiggles moved ~70% of the time (Table 1). In addition, almost no peripherin squiggle reversals were observed (Table 1). Overall, the results of these studies showed that the majority of peripherin particles and squiggles moved rapidly in the anterograde direction along neurites with fewer pauses and reversals than detected in either cell bodies or growth cones.

Mechanisms underlying the motility of particles and squiggles

Previous studies have shown that the motility of the various structural forms of IF proteins are dependent upon MT (Prahlad et al., 2000; Prahlad et al., 1998; Shah et al., 2000; Yoon et al., 1998). Therefore, FRAP analyses were performed on GFP-peripherin-expressing PC12 cells grown in DM for 48 hours and treated with colchicine for 15 minutes-2 hours (see Materials and Methods). Phase contrast images revealed that no significant neurite retraction occurred during the observation period, and no MT could be detected by immunofluorescence at 15 minutes after adding colchicine (data not shown). Time-lapse observations of bleach zones demonstrated that only ~23% (n=10) of the total fluorescence was recovered, even at 1 hour post-photobleaching (Fig. 5D). This recovery was much slower than that recorded for controls (Fig. 5A-C). In addition, there were no transient increases in fluorescence intensity (Fig. 5D1-D3), as no particles or

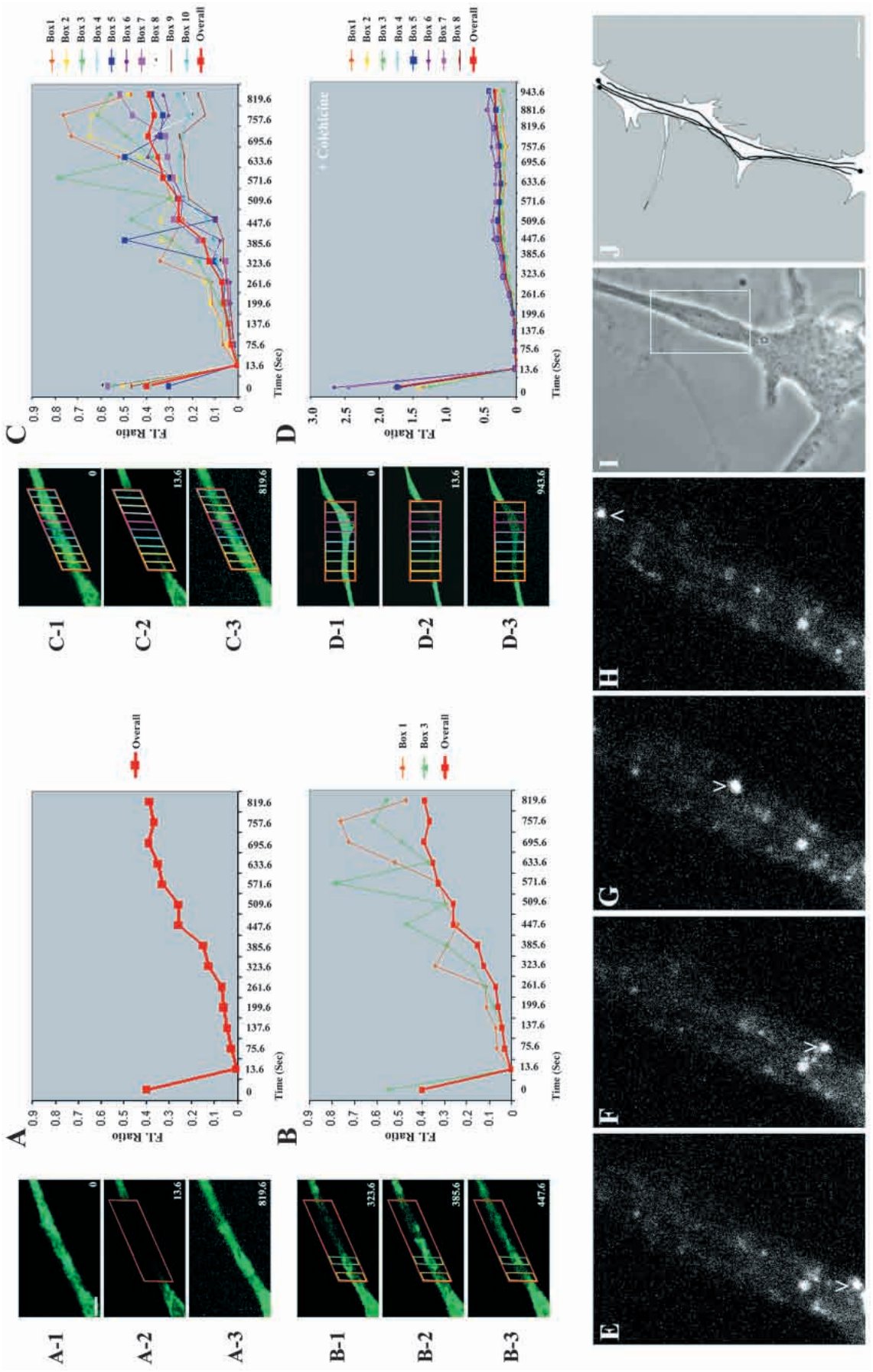
A
B
C
D
A-1
A-2
A-3
B-1
B-2
B-3
C-1
C-2
C-3
D-1
D-2
D-3
E
F
G
H
I
J
Overall
Box 1
Box 3
Box 1
Box 2
Box 3
Box 4
Box 5
Box 6
Box 7
Box 8
Box 9
Box 10
+ Colchicine
FL Ratio
Time (Sec)

Fig. 5. Particle and squiggle motility contribute to fluorescence recovery after photobleaching (FRAP). A bleach zone (areas denoted by red outlines) was made along the length of a neurite in a GFP-peripherin-expressing PC12 cell cultured in DM for 48 hours. Photobleaching required ~14 seconds (see A2, C2). Fluorescence recovery was subsequently monitored by determining the fluorescence intensity ratio (F.I.; see Materials and Methods) within this region by capturing images at ~60 seconds intervals for ~800 seconds. Using this ratio to determine the overall rate of fluorescence recovery, it was observed that the $t_{1/2}$ (see A) for peripherin in this cell is ~400 seconds (also see A1-3, which represent the region prior to photobleaching, immediately following photobleaching at ~14 seconds and ~800 seconds after bleaching). The F.I. ratio was also determined for two subdivisions of the same region indicated by the large red box [B; B1-3 (subdivisions outlined in orange and green) at ~333, 385 and 448 seconds]. Using this more detailed analysis of recovery, transient peaks in the F.I. ratio were observed (see green and orange lines in B). These peaks were attributable to the rapid movements of bright squiggles and particles seen moving into and out of the bleach zone throughout the recovery period. In C, the same neurite has been separated into 10 subdivisions, including those depicted in B, each indicated by a different color on the graph (also see C1-3). This resulted in the complex series of peaks detected within the bleach zone during recovery. In addition, FRAP analysis was performed in a similar manner on another neurite of a PC12 cell grown in DM for 48 hours and then in DM containing 5 μg/ml colchicine for 30-45 minutes (D-1 to D-3). There was very little recovery up to 930 seconds after photobleaching (compare A with D). Interestingly, there was almost no fluctuation observed in the F.I. ratio and no particles or squiggles were observed to move within the bleach zone. Images E-H show GFP-peripherin particle movements through a photobleached area of the neurite shown in the phase image (I). Images were taken at 5 second intervals following photobleaching. The particle marked with an arrowhead moved in an anterograde direction at rates that ranged from 0.31-1.0 μm/second (also see Movie 2, available at jcs.biologists.org/supplemental). Diagrams of three trajectories of GFP-peripherin squiggles were made from another neurite (J). Black dots represent the beginning of squiggle tracks. Reversals of particles and squiggles were very infrequent within neurites of differentiated cells. E-H, Bar, 2 μm; I, J, Bars, 5 μm.

squiggles could be detected traversing the bleach zones. Fixation and staining after photobleaching demonstrated that a dense array of peripherin IF remained in the bleach zone (data not shown; Materials and Methods). These observations suggest that the movements of particles and squiggles into bleach zones are required for normal fluorescence recovery.

Immunofluorescence was employed to determine the relationships between peripherin particles, squiggles and MT in the growth cones of non-transfected PC12 cells after 4 hours in DM. These studies showed that the majority of particles (78%; *n*=96) and squiggles (88%; *n*=184) present in several different growth cones were associated with MT (Fig. 6A-D).

The findings that MT are required for the motility of peripherin particles and squiggles suggested that MT-associated motors provide the motive force for their movements. Immunofluorescence observations of PC12 cells replated in DM for 0.5-12 hours showed that the majority of peripherin particles (79%; *n*=154) and squiggles (80%; *n*=137) were associated with conventional kinesin (Fig. 6E). Similar results were obtained after 24-72 hours in DM in the peripheral regions of cell bodies and growth cones (data not shown). Since retrograde movements were also detected, the relationship between dynein, dynactin and peripherin was determined. This involved double labeling with anti-peripherin and dynein intermediate chain, or anti-peripherin and either p50 (dynamitin) or p150^{Glued}. The results were indistinguishable for each of these antibodies (see, for example, Fig. 6F). Approximately 73% (*n*=250) of the peripherin particles and ~86% (*n*=300) of the squiggles were closely associated with dynein and dynactin (Fig. 6F).

Since individual GFP-peripherin particles and squiggles were observed to move in one direction and then rapidly reverse, it was of interest to further determine the relationships between peripherin, dynein, dynactin and kinesin. Double label immunofluorescence analyses of 15 different growth cones in GFP-peripherin-expressing cells revealed that ~40% of the particles (*n*=423) were associated with both kinesin and dynein (Fig. 7A-F); ~25% were associated only with dynein (Fig. 7A,C,E); ~21% associated only with kinesin (Fig. 7A,B,D); and ~14% did not appear to associate with either motor (Fig. 7F). In addition, ~56% of the squiggles (*n*=300) were associated with both motors, ~15% were associated with dynein only, ~18% were associated with kinesin only and ~11% did not appear to associate with either motor.

To be certain that the associations observed among peripherin, kinesin and/or dynein were not random, statistical analyses were carried out as described (see Materials and Methods). Briefly, double- and triple-labeled fluorescence images of PC12 cells grown in DM for 2-4 hours were used for analyses. The total areas of randomly selected cytoplasmic regions as well as the total number and average size of peripherin, kinesin and/or dynein particles were determined. We also determined the actual number of peripherin particles that associated with kinesin and/or dynein. Using these values, we calculated that the probability of the associations observed between peripherin and kinesin, between peripherin and dynein, and among peripherin, kinesin and dynein by chance alone was less than 1 in 10,000. On the basis of these analyses, we are confident that a significant population of peripherin particles is associated with both kinesin and dynein.

At higher resolution, platinum replica immunogold electron microscopy of cytoskeletal preparations that preserve the integrity of IF and MT (Helfand et al., 2002) confirmed the observation that perpherin particles were closely associated with MT in the central domains of growth cones (Fig. 8). In addition, in double-labeled preparations, the clusters of gold particles seen with the peripherin antibody frequently colocalized with anti-kinesin (Fig. 8A-C) or anti-dynein (Fig. 8D-F) antibodies.

We also determined whether kinesin, dynein and dynactin were present in PC12 IF-enriched cytoskeletal preparations at 72 hours after replating in DM (see Materials and Methods). Immunoblot analyses of these preparations revealed, in addition to the major peripherin band, the presence of kinesin heavy chain and components of the dynein and dynactin complexes including IC, LIC1 and 2, HC, dynamitin (p50), p150^{Glued} and Arp-1 (Fig. 9; Materials and Methods).

Dynein, dynactin and kinesin are required for maintaining peripherin IF organization

The relationships between peripherin, MT and their associated

motors were also studied by disrupting the activities of conventional kinesin and cytoplasmic dynein in PC12 cells. To test whether kinesin is required to maintain the organization of the peripherin IF network, differentiated PC12 cells (48 hours in DM) were microinjected with either kinesin antibody (0.75 mg/ml) or, as a control, with non-immune serum (see Materials and Methods) (Prahlad et al., 1998). Cells were processed for immunofluorescence with peripherin antibody 0.5-4 hours after microinjection. In every cell injected with kinesin antibody (n=35) virtually all of the peripherin was located in the juxtanuclear region within the cell body (Fig. 10C,D). Very few, if any, peripherin IF, particles or squiggles could be detected in neurites. In controls, typical peripherin networks were seen (Fig. 10A,B). We observed no significant retraction of PC12 processes during these time intervals after microinjection (see Materials and Methods).

To determine the role of dynein in peripherin IF network organization, PC12 cells grown for 24-48 hours in DM were transfected with myc-dynamitin cDNA [see Materials and Methods (Echeverri et al., 1996; Helfand et al., 2002)]. Forty-eight hours later, the cells were fixed and processed for double label immunofluorescence using antibodies against peripherin and c-myc. Observations of control mock-transfected cells revealed typical peripherin

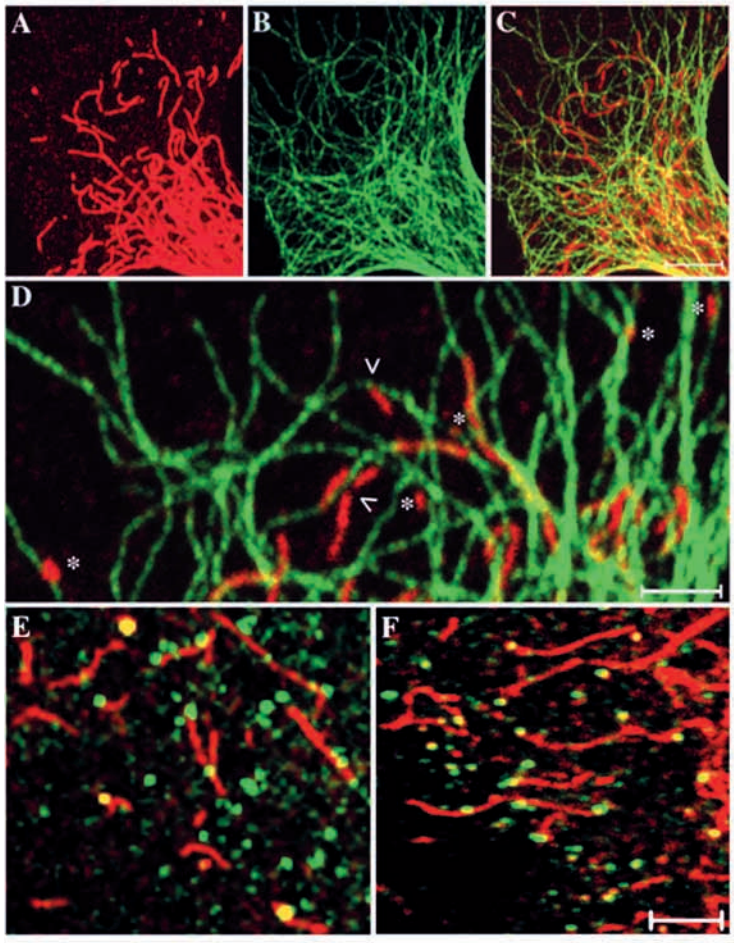

Fig. 6. Peripherin association with microtubules and motors. Peripherin particles and squiggles are closely associated with microtubules (MT) in the growth cone of a PC12 cell in DM for 4 hours. (A-D) Double label immunofluorescence. (A) peripherin (red); (B) microtubules (green); (C) overlay. D is a magnified view of the peripheral region of the growth cone shown in C. (E) Overlay of a double-labeled immunofluorescence preparation showing the association (yellow) between peripherin particles and squiggles (red) and kinesin (green). (F) Overlay of double label immunofluorescence preparation showing the association (yellow) between peripherin (red) and dynein IC (green). Bars, 2 μm.

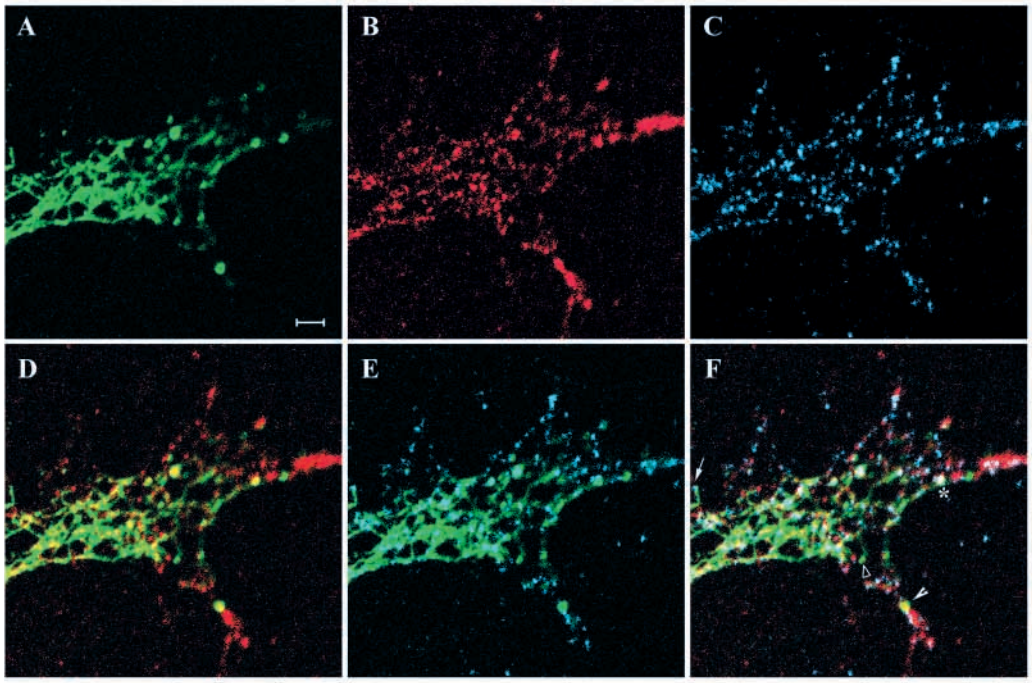

Fig. 7. Individual peripherin structures can associate with both motors. GFP-peripherin-transfected PC12 cells were plated in DM for 4 hours and then processed for indirect immunofluorescence using anti-kinesin heavy chain (red) and dynein heavy chain (blue). It was determined that the majority of particles and squiggles associate with both kinesin and dynein (A,B,C, see asterisk in F). Some of these peripherin structures associate only with dynein (A,C,E, see arrow in F), others associate only with kinesin (A,B,D, see filled arrowhead in F), and a small percentage do not appear to associate with either motor (see open arrowhead). Bar, 5 μm.

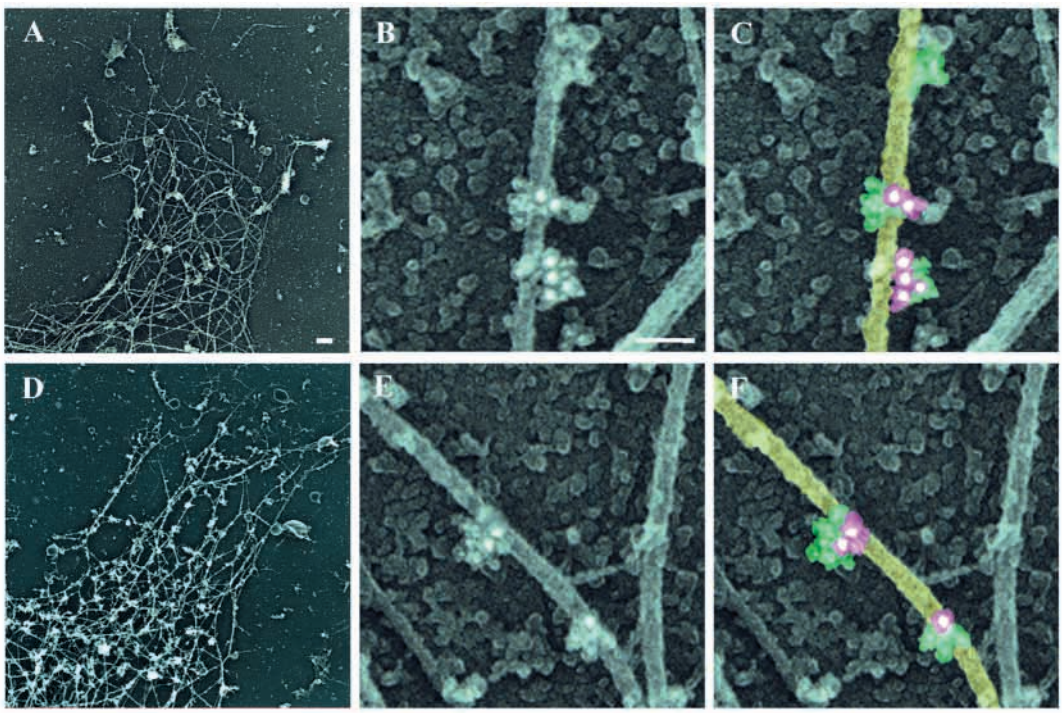

Fig. 8. Ultrastructural analysis of peripherin particles within growth cones. PC12 cells plated in DM for 4 hours were processed for platinum replica immunogold electron microscopy using a rabbit polyclonal peripherin antibody, a mouse monoclonal kinesin heavy chain antibody and/or a mouse monoclonal dynein intermediate chain antibody. Secondary antibodies were 10 nm gold-conjugated anti-rabbit and 18 nm gold-conjugated anti-mouse antibodies. In the central domain of the growth cone, many particles associated with MT and their associated motors. A-C demonstrate kinesin and peripherin association. C is a color overlay showing peripherin (green), kinesin (pink) and MT (yellow). D-F show an association between peripherin and dynein. F is a color overlay showing peripherin (green), dynein (pink) and MT (yellow). A and D, Bar, 600 nm; B,C,E,F, Bar, 100 nm.

networks (Fig. 10E,F). Cells over-expressing dynamitin displayed a dramatic decrease in peripherin in the perinuclear area (Fig. 10E,F). The majority of the peripherin was concentrated in the distal regions of neurites and in some cases near the surface of the cell body. On the basis of these observations and those described above for kinesin, it appears that both plus-end- and minus-end-directed MT-associated motors are required for the maintenance of normal peripherin networks in differentiated PC12 cells.

Discussion

Pioneering studies using radioisotope labeling in vivo have demonstrated that the majority of neural IF proteins move slowly in an anterograde direction at average rates of 0.0002-0.0007 μm/minute [0.3-1.0 mm/day (Hoffman and Lasek, 1975; Lasek and Hoffman, 1976)]. However, recent results obtained from direct observations of GFP-NF-M- and GFP-NF-H-transfected sympathetic neurons have revealed that short NF can be transported bi-directionally in axons at much faster speeds averaging ~0.4-0.6 μm/second (Roy et al., 2000; Wang et al., 2001; Wang et al., 2000). Even though these rates are consistent with fast transport, the majority of NF reported in these experiments moved only ~20% of the time, thereby maintaining an overall slow transport rate. In contrast, the analysis of the motile properties of the peripherin particles reported here demonstrates that they move rapidly ~75% of the time in differentiated cells. The average anterograde rates of peripherin particle and squiggle motility are equivalent to ~29

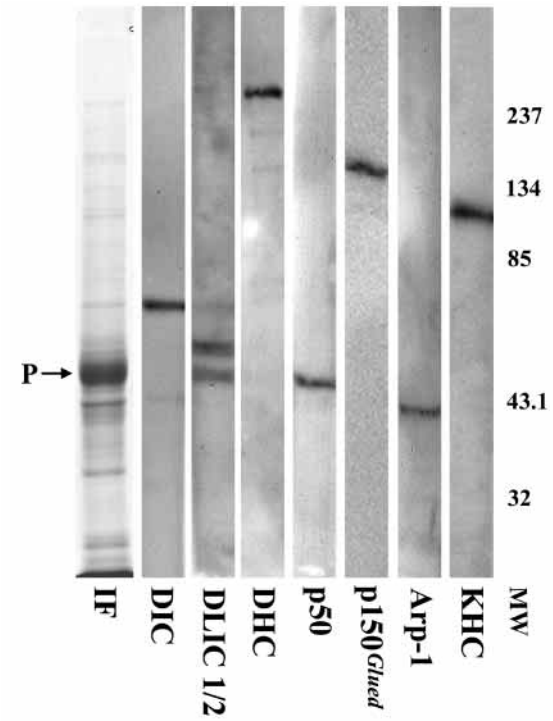

Fig. 9. IF-enriched cytoskeletons contain motor subunits. Lane 'IF' is a Coomassie stain showing that peripherin (P) is the major protein present in IF-enriched cytoskeletal preparations. Immunoblot analysis of these same preparations shows that kinesin and many of the components of dynein and dynactin are present. MW indicates molecular weight standards. DIC, dynein intermediate chain; DLIC1 /2, dynein light intermediate chain isoforms 1 and 2; DHC, dynein heavy chain; p50, dynamitin; Arp-1, actin related protein-1; KHC, kinesin heavy chain.

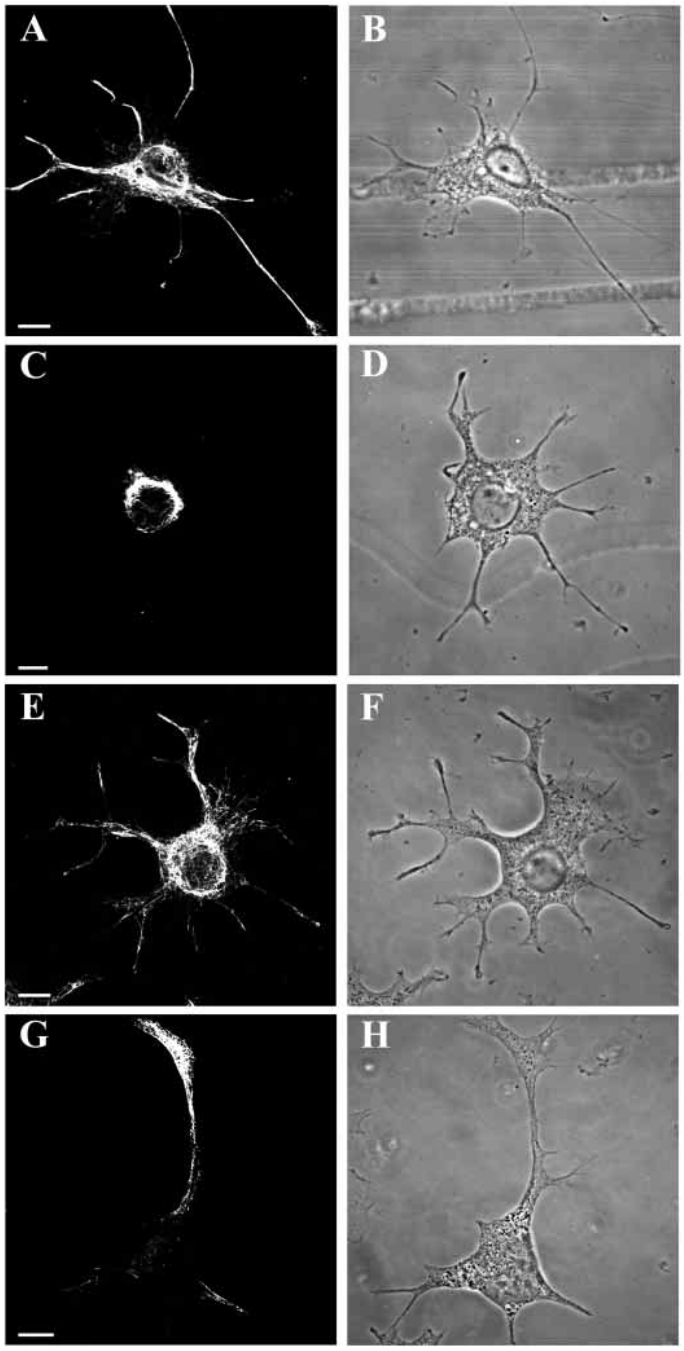

Fig. 10. Disruption of motors alters the distribution of peripherin. PC12 cells grown on locator coverslips in DM for 48 hours were microinjected with kinesin heavy chain antibody (C,D) or as a control, with non-immune serum (A,B), and then processed for immunofluorescence using peripherin antibody at 0.5-4 hours post-injection. Control cells displayed normal peripherin networks (A). In cells injected with kinesin antibody the peripherin was almost exclusively located in the cell body (C). B and D are phase images of the same injected cells.PC12 cells were also transfected with myc-dynamitin cDNA (G) or mock transfected (E) and processed for immunofluorescence with peripherin and c-myc (data not shown) antibodies, 48 hours post-transfection. Dynamitin-expressing cells showed peripherin staining almost exclusively in the peripheral regions of the cell body and distal regions of neurites (G). Mock-transfected cells displayed peripherin networks that were typical of well-differentiated cells. Phase contrast (F,H). Bars, 10 μm.

mm/day (0.33 μm/second) and ~27 mm/day (0.31 μm/second), respectively. These averages lie between those reported for fast and slow axonal transport in whole animal studies (Lasek and Hoffman, 1976). However, a more detailed analysis of peripherin movements within the neurites of differentiated PC12 cells reveals that ~18% of the particles and ~26% of the squiggles moved within the range of 0.5-1.54 μm/second, which extrapolates to 50-133 mm/day (see Table 1). Thus, a subpopulation of peripherin particles and squiggles move at rates similar to those recorded for mitochondria (Brown, 2000). Although isotope tracing methods suggest that the bulk of cytoskeletal IF protein transport is very slow (Lasek and Hoffman, 1976), there is also a small radioactive fraction that moves at rates between 72-144 mm/day (Lasek et al., 1993). These rates are remarkably similar to those calculated for the fastest moving peripherin particles and squiggles, and therefore they may represent the same population of cytoskeletal components. It is therefore possible that the rapid movement of even a small population of particles and squiggles provides a mechanism for the targeted and timely delivery of the structural subunits required for the maintenance and turnover of IF networks in all regions of peripheral neurons. In support of this there is evidence that non-filamentous particles can be directly incorporated into IF networks, as well as converted into short IF (Chou et al., 2001; Miller et al., 1991; Prahlad et al., 1998; Vikstrom et al., 1989). Furthermore, it is possible and even likely that similar rapidly moving subpopulations of unpolymerized tubulin and actin may exist. For example, recent experiments suggest that some forms of tubulin are associated with kinesin and move at speeds comparable to those recorded for neural IF (Terada et al., 2000; Wang and Brown, 2002).

In BHK-21 fibroblasts, and in the cell bodies and growth cones of PC12 cells, particles and squiggles move ~50% of the time (see Table 1). However, PC12 neurites contain particles and squiggles that spend a significantly greater proportion of their time moving (~75%). In addition, the motility of these structures within neurites appears to be more directed when compared to their motility within cell bodies and growth cones. This is supported by the findings that there are very few reversals of particle and squiggle movements observed within neurites (Table 1). Taken together, it appears that there are specific mechanisms within neurites that are not present within fibroblasts, neuronal growth cones or cell bodies which enhance IF motility. Possible explanations for these alterations in motile behavior may lie in the changes in the phosphorylation states of IF and/or motor proteins known to take place specifically within neurites (Jung et al., 2000a; Lee and Hollenbeck, 1995; Lee et al., 1986; Nixon et al., 1987; Oblinger et al., 1987; Pfister et al., 1996; Salata, 2001; Sternberger and Sternberger, 1983; Yabe et al., 2000).

Our results show that IF protein is present within all regions of growth cones. As mentioned above, the behavior of peripherin particles and squiggles within the central domain of growth cones, known to contain both MT and actin (Mueller, 1999), was similar to that described in cell bodies. In addition, this is the first study to detect IF protein in the form of non-filamentous particles in the peripheral domain of growth cones. This domain is defined by its lack of MT and its enriched actin content (Mueller, 1999). Preliminary observations of GFP-peripherin particles within the peripheral domain reveals that

the vast majority move in a retrograde direction at much slower rates (data not shown). This suggests that these movements may be linked to the actomyosin system. Further support for this possibility comes from the observation that peripherin can associate with actin through myosin Va, a processive actin-associated motor that is enriched in growth cones (Rao et al., 2002; Wolff et al., 1999). Therefore, it is possible that different structural forms of peripherin can also be transported by the actomyosin system.

As indicated above, the range of rapid movements recorded for the type III IF peripherin particles and squiggles in PC12 cells reported in this study and for the short type IV IF (NF) described in cultured sympathetic nerve cells (Roy et al., 2000; Wang et al., 2000) are very similar. In contrast, the overall distances traveled by these different types of neural IF proteins can be explained by their dramatically different pause times. One explanation for this difference may be related to the structure of the triplet proteins comprising the short motile NF observed in sympathetic neurons. Both NF-M and NF-H have unusually long highly charged C-terminal tails that project from the core IF structure (Hirokawa et al., 1997; Hisanaga and Hirokawa, 1988). It has been suggested that these domains, and their modification by phosphorylation, promote filament stability and modify NF transport in axons by regulating interactions with MT and MT-dependent motors (Chen et al., 2000; Hisanaga and Hirokawa, 1988; Jung et al., 2000b; Nakagawa et al., 1995; Yabe et al., 2001b; Yabe et al., 1999). Therefore, it is possible that the tail domains of NF-M and NF-H could be involved, either actively or passively, in determining pause intervals, thereby influencing the total distances traveled by NF. In support of this possibility, it has been shown that the initiation of NF-H expression during postnatal development is coincident with a decrease in the overall rates of axonal transport (Cote et al., 1993; Marszalek et al., 1996; Willard and Simon, 1983). Furthermore, the disruption of NF-M or NF-H genes in mice accelerates axonal transport of NF-L (Jacomy et al., 1999; Zhu et al., 1998). On the basis of these observations, it appears that the rapid movements of peripherin particles and squiggles may be related to the absence of the long highly charged tail domains that are characteristic of mature NF.

It is also possible that particulate non-filamentous forms of NF triplet proteins, similar to those described for vimentin IF precursors (Prahlad et al., 1998), and the peripherin particles described in this study, could move at fast transport rates. In support of this possibility, rapidly moving NF particles containing the triplet proteins have been described in squid axoplasm (Prahlad et al., 2000), dorsal root ganglion neurons and neuroblastoma cells (Yabe et al., 2001a). Unfortunately, none of these studies calculated the pause times required to determine whether the NF particles are components of a rapid transport system.

FRAP studies of the peripherin network along neurites in differentiated PC12 cells demonstrate that the $t_{1/2}$ for fluorescence recovery is almost identical to that recorded for another member of the type III IF family, vimentin (Yoon et al., 1998). Interestingly, the fluorescence recovery of both peripherin and vimentin IF slow down significantly in the absence of microtubules [see Fig. 5D (Yoon et al., 1998)]. However, the recovery of GFP-peripherin fluorescence is even more sensitive to MT inhibitors, as only ~23% recovery was recorded at 1 hour post-photobleaching (see Fig. 5D). In addition, under these conditions, no peripherin particle or squiggle motility was observed in bleach zones made along the length of neurites. These observations suggest that the majority of subunit exchange required for normal fluorescence recovery along neurites may be dependent on the MT-based transport of IF precursors such as particles and squiggles. It is also possible that the partial recovery (~23%) detected under these conditions may be related to an actomyosin-based transport system for delivering IF precursors. In support of this, actomyosin-based transport has been reported in nerve cells (Evans and Bridgman, 1995; Tabb et al., 1998).

Two theories have been proposed to describe the mechanisms of neural IF protein transport within axons. The subunit transport theory holds that neural IF are transported along MT as oligomeric complexes (Hirokawa et al., 1997). The second theory states that neural IF are transported within axons as fully assembled polymers (Bass and Brown, 1997). Our observations of live cells suggest that aspects of both theories are correct as we have demonstrated that both non-filamentous (particles) and short neural IF (squiggles) can be transported in a MT-dependent manner within all regions of PC12 cells. We have also demonstrated that the majority of particles and squiggles associate with both conventional kinesin and cytoplasmic dynein (see Fig. 7). This finding complements other studies that have demonstrated both kinesin- and dynein-dependent transport of type III IF proteins in fibroblasts and type IV NF proteins in neurons (Helfand et al., 2002; Prahlad et al., 2000; Prahlad et al., 1998; Shah et al., 2000; Yabe et al., 1999). It is also of interest to note that although many of the peripherin particles are associated with both kinesin and dynein, the majority of movements are anterograde. This may reflect specific modifications that regulate MT-associated motor components (Lee and Hollenbeck, 1995; Morfini et al., 2002; Reese and Haimo, 2000; Salata et al., 2001).

The finding that neural IF proteins are transported along MT by motor proteins also has important implications for understanding numerous human neurodegenerative disorders such as amyotrophic lateral sclerosis (ALS) and Parkinson's Disease (PD). The pathological hallmarks of these diseases are abnormal accumulations of neural IF within axons and cell bodies (Gotow, 2000; Julien and Mushynski, 1998). Our studies suggest that similar accumulations can occur following the disruption of either kinesin or dynein function in PC12 cells. This is further supported by recent findings demonstrating progressive neuronal degeneration in transgenic mice that overexpress dynamitin in mature motor neurons (LaMonte et al., 2002). The motor neurons in these mice display large aggregates of NF, and this is coincident with the development of motor neuron disease (LaMonte et al., 2002).

In conclusion, our study demonstrates that non-filamentous, non-membrane-bound particles and short filaments containing peripherin move along neurites at rates consistent with rapid transport. It therefore appears likely that a subpopulation of cytoskeletal IF proteins can move at rapid rates along axons, providing a mechanism for the timely turnover, replacement and repair of cytoskeletal components within the most distal reaches of neurons.

The authors would like to thank Satya Khuon for her technical assistance. We would also like to thank Guenter Albrecht-Buehler for his time and expert assistance in determining the statistical analyses. This study was supported by NIGMS MERIT Grant (GM 36806) awarded to R.D.G. and a F30 NRSA (AA 13470) to B.T.H.

References

Bass, P. W. and Brown, A. (1997). Slow axonal transport: the polymer transport model. *Trends Cell Biol.* **7**, 380-384.

Brody, B. A., Ley, C. A. and Parysek, L. M. (1989). Selective distribution of the 57kDa neural intermediate filament protein in the rat CNS. *J. Neurosci.* **9**, 2391-2401.

Brown, A. (2000). Slow axonal transport: stop and go traffic in the axon. *Nat. Rev. Mol. Cell Biol.* **1**, 153-156.

Chen, J., Nakata, T., Zhang, Z. and Hirokawa, N. (2000). The C-terminal tail domain of neurofilament protein-H (NF-H) forms the crossbridges and regulates neurofilament bundle formation. *J. Cell Sci.* **113**, 3861-3869.

Chou, Y. H., Helfand, B. T. and Goldman, R. D. (2001). New horizons in cytoskeletal dynamics: transport of intermediate filaments along microtubule tracks. *Curr. Opin. Cell Biol.* **13**, 106-109.

Cote, F., Collard, J. F. and Julien, J. P. (1993). Progressive neuronopathy in transgenic mice expressing the human neurofilament heavy gene: a mouse model of amyotrophic lateral sclerosis. *Cell* **73**, 35-46.

Echeverri, C. J., Paschal, B. M., Vaughan, K. T. and Vallee, R. B. (1996). Molecular characterization of the 50-kD subunit of dynactin reveals function for the complex in chromosome alignment and spindle organization during mitosis. *J. Cell Biol.* **132**, 617-633.

Escurat, M., Djabali, K., Gumpel, M., Gros, F. and Portier, M. M. (1990). Differential expression of two neuronal intermediate-filament proteins, peripherin and the low-molecular-mass neurofilament protein (NF-L), during the development of the rat. *J. Neurosci.* **10**, 764-784.

Evan, G. I., Lewis, G. K., Ramsay, G. and Bishop, J. M. (1985). Isolation of monoclonal antibodies specific for human c-myc proto-oncogene product. *Mol. Cell. Biol.* **5**, 3610-3616.

Evans, L. L. and Bridgman, P. C. (1995). Particles move along actin filament bundles in nerve growth cones. *Proc. Natl. Acad. Sci. USA* **92**, 10954-10958.

Fujita, K., Lazarovici, P. and Guroff, G. (1989). Regulation of the differentiation of PC12 pheochromocytoma cells. *Environ. Health Perspect.* **80**, 127-142.

Gotow, T. (2000). Neurofilaments in health and disease. *Med Electron Microsc* **33**, 173-199.

Hammerschlag, R., Cyr, J. L. and Brady, S. T. (1994). Axonal transport and the neuronal cytoskeleton. In *Basic Neurochemistry: Molecular, Cellular, and Medical Aspects*, 5th edition (ed. G. J. Siegal), pp. 545-571. New York: Raven Press, Ltd.

Helfand, B. T., Mikami, A., Vallee, R. B. and Goldman, R. D. (2002). A requirement for cytoplasmic dynein and dynactin in intermediate filament network assembly and organization. *J. Cell Biol.* **157**, 795-806.

Hirokawa, N., Terada, S., Funakoshi, T. and Takeda, S. (1997). Slow axonal transport – the subunit transport model. *Trends Cell Biol* **7**, 384-388.

Hisanaga, S. and Hirokawa, N. (1988). Structure of the peripheral domains of neurofilaments revealed by low angle rotary shadowing. *J. Mol. Biol.* **202**, 297-305.

Ho, C. L., Martys, J. L., Mikhailov, A., Gundersen, G. G. and Liem, R. K. (1998). Novel features of intermediate filament dynamics revealed by green fluorescent protein chimeras. *J. Cell Sci.* **111**, 1767-1778.

Hoffman, P. N. and Lasek, R. J. (1975). The slow component of axonal transport. Identification of major structural polypeptides of the axon and their generality among mammalian neurons. *J. Cell Biol.* **66**, 351-366.

Jacomy, H., Zhu, Q., Couillard-Despres, S., Beaulieu, J. M. and Julien, J. P. (1999). Disruption of Type IV intermediate filament network in mice lacking the neurofilament medium and heavy subunits. *J. Neurochem.* **73**, 972-984.

Julien, J. P. and Mushynski, W. E. (1998). Neurofilaments in health and disease. *Prog. Nucleic Acid Res. Mol. Biol.* **61**, 1-23.

Jung, C., Yabe, J. T., Lee, S. and Shea, T. B. (2000a). Hypophosphorylated neurofilament subunits undergo axonal transport more rapidly than more extensively phosphorylated subunits in situ. *Cell Motil. Cytoskeleton* **47**, 120-129.

Jung, C., Yabe, J. T. and Shea, T. B. (2000b). C-terminal phosphorylation of the high molecular weight neurofilament subunit correlates with decreased neurofilament axonal transport velocity. *Brain Res.* **856**, 12-19.

Laemmli, U. K. (1970). Cleavage of structural protiens during the assembly of the head of bacteriophage T4. *Nature* **227**, 680-685.

LaMonte, B. H., Wallace, K. E., Holloway, B. A., Shelly, S. S., Ascano, J., Tokito, M., van Winkle, T., Howland, D. S. and Holzbaur, E. L. (2002). Disruption of dynein/dynactin inhibits axonal transport in motor neurons causing late-onset progressive degeneration. *Neuron* **34**, 715-727.

Lasek, R. J. and Hoffman, P. N. (1976). The neuronal cytoskeleton, axonal transport and axonal growth. *Cold Spring Harbor Conf. Cell Prolif.* **3**, 1021-1049.

Lasek, R. J., Paggi, P. and Katz, M. J. (1993). The maximum rate of neurofilament transport in axons: a view of molecular transport mechanisms continuously engaged. *Brain Res* **616**, 58-64.

Lee, K. D. and Hollenbeck, P. J. (1995). Phosphorylation of kinesin in vivo correlates with organelle association and neurite outgrowth. *J. Biol. Chem.* **270**, 5600-5605.

Lee, V. M., Carden, M. J. and Trojanowski, J. Q. (1986). Novel monoclonal antibodies provide evidence for the in situ existence of a nonphosphorylated form of the largest neurofilament subunit. *J. Neurosci.* **6**, 850-858.

Marszalek, J. R., Williamson, T. L., Lee, M. K., Xu, Z., Hoffman, P. N., Becher, M. W., Crawford, T. O. and Cleveland, D. W. (1996). Neurofilament subunit NF-H modulates axonal diameter by selectively slowing neurofilament transport. *J. Cell Biol.* **135**, 711-724.

Miller, R. K., Vikstrom, K. and Goldman, R. D. (1991). Keratin incorporation into intermediate filament networks is a rapid process. *J. Cell Biol.* **113**, 843-855.

Morfini, G., Szebenyi, G., Elluru, R., Ratner, N. and Brady, S. T. (2002). Glycogen synthase kinase 3 phosphorylates kinesin light chains and negatively regulates kinesin-based motility. *EMBO J.* **21**, 281-293.

Mueller, B. K. (1999). Growth cone guidance: first steps towards a deeper understanding. *Annu. Rev. Neurosci.* **22**, 351-388.

Nakagawa, T., Chen, J., Zhang, Z., Kanai, Y. and Hirokawa, N. (1995). Two distinct functions of the C-terminal tail domain of NF-M upon neurofilament assembly: cross-bridge formation and longitudinal elongation of filaments. *J. Cell Biol.* **129**, 411-429.

Nixon, R. A. (1993). The regulation of neurofilament protein dynamics by phosphorylation: clues to neurofibrillary pathobiology. *Brain Pathol.* **3**, 29-38.

Nixon, R. A., Lewis, S. E. and Marotta, C. A. (1987). Post-translational modification of neurofilament proteins by phosphate during axoplasmic transport in retinal ganglion cell neurons. *J. Neurosci.* **7**, 1145-1158.

Oblinger, M. M., Brady, S. T., McQuarrie, I. G. and Lasek, R. J. (1987). Cytotypic differences in the protein composition of the axonally transported cytoskeleton in mammalian neurons. *J. Neurosci.* **7**, 453-462.

Parysek, L. M. and Goldman, R. D. (1988). Distribution of a novel 57kDa intermediate filament (IF) protein in the nervous system. *J. Neurosci.* **8**, 555-563.

Pfister, K. K., Salata, M. W., Dillman, J. F., 3rd, Vaughan, K. T., Vallee, R. B., Torre, E. and Lye, R. J. (1996). Differential expression and phosphorylation of the 74-kDa intermediate chains of cytoplasmic dynein in cultured neurons and glia. *J. Biol. Chem.* **271**, 1687-1694.

Prahlad, V., Yoon, M., Moir, R. D., Vale, R. D. and Goldman, R. D. (1998). Rapid movements of vimentin on microtubule tracks: kinesin-dependent assembly of intermediate filament networks. *J. Cell Biol.* **143**, 159-170.

Prahlad, V., Helfand, B. T., Langford, G. M., Vale, R. D. and Goldman, R. D. (2000). Fast transport of neurofilament protein along microtubules in squid axoplasm. *J. Cell Sci.* **113**, 3939-3946.

Rao, M. V., Engle, L. J., Mohan, P. S., Yuan, A., Qiu, D., Cataldo, A., Hassinger, L., Jacobsen, S., Lee, V. M., Andreadis, A. et al. (2002). Myosin Va binding to neurofilaments is essential for correct myosin Va distribution and transport and neurofilament density. *J. Cell Biol.* **159**, 279-290.

Reese, E. L. and Haimo, L. T. (2000). Dynein, dynactin, and kinesin II's interaction with microtubules is regulated during bidirectional organelle transport. *J. Cell Biol.* **151**, 155-166.

Roy, S., Coffee, P., Smith, G., Liem, R. K., Brady, S. T. and Black, M. M. (2000). Neurofilaments are transported rapidly but intermittently in axons: implications for slow axonal transport. *J. Neurosci.* **20**, 6849-6861.

Salata, M. W., Dillman, J. F., 3rd, Lye, R. J. and Pfister, K. K. (2001). Growth factor regulation of cytoplasmic dynein intermediate chain subunit expression preceding neurite extension. *J. Neurosci. Res.* **65**, 408-416.

Shah, J. V., Flanagan, L. A., Janmey, P. A. and Leterrier, J. F. (2000). Bidirectional translocation of neurofilaments along microtubules mediated in part by dynein/dynactin. *Mol. Biol. Cell* **11**, 3495-3508.

Spector, D. L., Goldman, R. D. and Leinwand, L. A. (1997). Nonimmunological fluorescent labeling of cellular structures. In *Cells: A Laboratory Manual*. Vol. 3 (ed. D. L. Spector, R. D. Goldman and L. A. Leinwand), pp. 101.1-101.12. New York: Cold Spring Harbor Laboratory Press.

Sternberger, L. A. and Sternberger, N. H. (1983). Monoclonal antibodies distinguish phosphorylated and nonphosphorylated forms of neurofilaments in situ. *Proc. Natl. Acad. Sci. USA* **80**, 6126-6130.

Svitkina, T. M., Verkhovsky, A. B. and Borisy, G. G. (1995). Improved procedures for electron microscopic visualization of the cytoskeleton of cultured cells. *J. Struct. Biol.* **115**, 290-303.

Tabb, J. S., Molyneaux, B. J., Cohen, D. L., Kuznetsov, S. A. and Langford, G. M. (1998) Transport of ER vesicles on actin filaments in neurons by myosin V. *J. Cell Sci.* **111**, 3221-3234.

Terada, S., Kinjo, M. and Hirokawa, N. (2000). Oligomeric tubulin in large transporting complex is transported via kinesin in squid giant axons. *Cell* **103**, 141-155.

Towbin, H., Staehelin, T. and Gordon, J. (1979). Electrophoretic transfer of proteins from polyacrylamide gels to nitrocellulose sheets: procedure and some applications. *Proc. Natl. Acad. Sci. USA* **76**, 4350-4354.

Troy, C. M., Brown, K., Greene, L. A. and Shelanski, M. L. (1990a). Ontogeny of the neuronal intermediate filament protein, peripherin, in the mouse embryo. *Neuroscience* **36**, 217-237.

Troy, C. M., Muma, N. A., Greene, L. A., Price, D. L. and Shelanski, M. L. (1990b). Regulation of peripherin and neurofilament expression in regenerating rat motor neurons. *Brain Res.* **529**, 232-238.

Tynan, S. H., Gee, M. A. and Vallee, R. B. (2000). Distinct but overlapping sites within the cytoplasmic dynein heavy chain for dimerization and for intermediate chain and light intermediate chain binding. *J. Biol. Chem.* **275**, 32769-32774.

Verkhovsky, A. B. and Borisy, G. G. (1993). Non-sarcomeric mode of myosin II organization in the fibroblast lamellum. *J. Cell Biol.* **123**, 637-652.

Vikstrom, K. L., Borisy, G. G. and Goldman, R. D. (1989). Dynamic aspects of intermediate filament networks in BHK-21 cells. *Proc. Natl. Acad. Sci. USA* **86**, 549-553.

Wang, L. and Brown, A. (2001). Rapid intermittent movement of axonal neurofilaments observed by fluorescence photobleaching. *Mol. Biol. Cell* **12**, 3257-3267.

Wang, L. and Brown, A. (2002). Rapid movement of microtubules in axons. *Curr. Biol.* **12**, 1496-1501.

Wang, L., Ho, C. L., Sun, D., Liem, R. K. and Brown, A. (2000). Rapid movement of axonal neurofilaments interrupted by prolonged pauses. *Nat. Cell Biol.* **2**, 137-141.

Willard, M. and Simon, C. (1983). Modulations of neurofilament axonal transport during the development of rabbit retinal ganglion cells. *Cell* **35**, 551-559.

Wolff, P., Abreu, P. A., Espreafico, E. M., Costa, M. C., Larson, R. E. and Ho, P. L. (1999). Characterization of myosin V from PC12 cells. *Biochem. Biophys. Res. Commun.* **262**, 98-102.

Yabe, J. T., Pimenta, A. and Shea, T. B. (1999). Kinesin-mediated transport of neurofilament protein oligomers in growing axons. *J. Cell Sci.* **112**, 3799-3814.

Yabe, J. T., Jung, C., Chan, W. K. and Shea, T. B. (2000). Phospho-dependent association of neurofilament proteins with kinesin in situ. *Cell Motil. Cytoskeleton* **45**, 249-262.

Yabe, J. T., Chan, W. K., Chylinski, T. M., Lee, S., Pimenta, A. F. and Shea, T. B. (2001a). The predominant form in which neurofilament subunits undergo axonal transport varies during axonal initiation, elongation, and maturation. *Cell Motil. Cytoskeleton* **48**, 61-83.

Yabe, J. T., Chylinski, T., Wang, F. S., Pimenta, A., Kattar, S. D., Linsley, M. D., Chan, W. K. and Shea, T. B. (2001b). Neurofilaments consist of distinct populations that can be distinguished by C-terminal phosphorylation, bundling, and axonal transport rate in growing axonal neurites. *J. Neurosci.* **21**, 2195-2205.

Yoon, M., Moir, R. D., Prahlad, V. and Goldman, R. D. (1998). Motile properties of vimentin intermediate filament networks in living cells. *J. Cell Biol.* **143**, 147-157.

Yoon, K. H., Yoon, M., Moir, R. D., Khuon, S., Flitney, F. W. and Goldman, R. D. (2001). Insights into the dynamic properties of keratin intermediate filaments in living epithelial cells. *J. Cell Biol.* **153**, 503-516.

Zackroff, R. V., Idler, W. W., Steinert, P. M. and Goldman, R. D. (1982). In vitro reconstitution of intermediate filaments form mammalian neurofilament triplet polypeptides. *Proc. Natl. Acad. Sci. USA* **79**, 754-757.

Zhu, Q., Lindenbaum, M., Levavasseur, F., Jacomy, H. and Julien, J. P. (1998). Disruption of the NF-H gene increases axonal microtubule content and velocity of neurofilament transport: relief of axonopathy resulting from the toxin beta,beta'-iminodipropionitrile. *J. Cell Biol.* **143**, 183-193.